A novel syndrome with short stature, mandibular hypoplasia and osteoporosis may be associated with a *PRRT3* variant

Abhimanyu Garg[1], Hatem El-Shanti[2], Chao Xing[3], Zhengyang Zhou[4], Mousa Abujbara[5], Khadeja Al-Rashed[5], Mohammed El-Khateeb[5], Kamel Ajlouni[5], Anil K. Agarwal[1]

[1]From the Division of Nutrition and Metabolic Diseases, Department of Internal Medicine and the Center for Human Nutrition, UT Southwestern Medical Center, Dallas, Texas, USA.

[2]The National Center for Diabetes, Endocrinology and Genetics, and Department of Pediatrics, Carver College of Medicine, University of Iowa, Iowa City, IA, USA.

[3]McDermott Center for Human Growth and Development, Department of Population and Data Sciences, and Department of Bioinformatics, UT Southwestern Medical Center, Dallas, Texas, USA.

[4]Department of Biostatistics and Epidemiology, School of Public Health, University of North Texas Health Science Center, Fort Worth, Texas, USA.

[5]The National Center for Diabetes, Endocrinology and Genetics, and School of Medicine, University of Jordan, Amman, Jordan.

Key Words: PRRT3, progeroid syndrome, short stature, mandibular hypoplasia, growth hormone deficiency

Correspondence and Reprint Requests:

Abhimanyu Garg, M.D., Chief, Division of Nutrition and Metabolic Diseases, Department of Internal Medicine, UT Southwestern Medical Center, 5323 Harry Hines Blvd, K5.214, Dallas, TX 75390-8537.

E-mail: abhimanyu.garg@utsouthwestern.edu

Declaration of Interests: The authors declare no competing interests.

Financial Support: This work was supported by grant from the National Institutes of Health, R01-DK105448 and by the Southwestern Medical Foundation. The funding sources were not involved in study design, analysis and interpretation of data, writing of the paper, and in the decision to submit the article for publication.

Disclosure Summary: The authors have no financial relationships relevant to this article to disclose.

Precis:

A homozygous p.Glu394Lys variant in *PRRT3* may be associated with a novel autosomal recessive, progeroid syndrome with short stature, mandibular hypoplasia, osteoporosis, short eyebrows and mild GH deficiency.

Abstract

Context: Despite considerable progress in elucidating the molecular basis of various progeroid syndromes, some rare patients remain unexplained.

Objective: To elucidate molecular genetic basis of a novel autosomal recessive progeroid syndrome.

Participants: A 24-year-old male and his 18-year-old sister with short stature, mandibular hypoplasia, pointed nose, shrill voice, severe osteoporosis, and short eyebrows; and their unaffected siblings and parents belonging to a consanguineous Arab family.

Results: Using exome and Sanger sequencing, we report a novel homozygous p.Glu394Lys disease-causing variant in proline rich transmembrane protein 3 (*PRRT3*). PRRT3 belongs to the family of proline-rich proteins containing several repeats of a short proline-rich sequence but its function remains to be determined. Preliminary observations showing co-localization of Prrt3 and synaptophysin support its role in vesicle exocytosis. Consistent with the highest mRNA expression of *PRRT3* in the pituitary, both the patients had mild growth hormone deficiency but had near normal reproductive development.

Conclusions: We conclude that the homozygous p.Glu394Lys variant in *PRRT3* may be associated with a novel autosomal recessive, progeroid syndrome with short stature, mandibular hypoplasia, osteoporosis, short eyebrows and mild GH deficiency. Our findings extend the spectrum of progeroid syndromes and elucidate important functions of PRRT3 in human biology including secretion of growth hormone from the pituitary.

Introduction

In the last two decades, considerable progress has been made in identifying the molecular genetic basis of several progeroid syndromes, including Werner's syndrome (1), Hutchinson-Gilford progeria syndrome (2), atypical progeroid syndrome (3), mandibuloacral dysplasia (4, 5), mandibular hypoplasia, deafness and progeroid syndrome (6), and more recently, neonatal progeroid syndrome (7). These discoveries have revealed importance of several pathways in aging, such as those involved in the maintenance of nuclear membrane integrity by nuclear lamins A and C and in genomic stability by RECQ helicase enzymes and DNA/RNA polymerases, such as polymerase delta 1 catalytic subunit and polymerase (RNA) III Subunit A. Despite this progress, the molecular basis of some rare progeroid patients remains obscure. Here we report homozygous missense variant in *PRRT3* as the molecular genetic basis of a novel autosomal recessive progeroid syndrome.

Subjects and Methods

We ascertained two affected siblings belonging to a consanguineous Arab pedigree. This study was reviewed and approved by the Institutional Review Board of UT Southwestern Medical Center, Dallas, Texas. Both the affected subjects, their parents, and unaffected siblings provided written informed consent for participation in the current study.

Clinical features of the two affected subjects were as follows:

Patient J100.3: This 24-year-old male had poor weight gain, short stature and muscle weakness since age 6. He developed puberty at age 17 but had a high-pitched voice. His height was 156 cm (2.2 percentile, z-score -2.0 using data from https://tall.life/height-percentile-calculator-age-country/ for adult males in Jordan). At age 21, his body weight was 31.5 kg (Z score -8.5), body mass index (BMI) was 12.9 kg/m^2 (z score -9.5) and occipito-frontal circumference was 51.5 cm (z score -2.4) denoting microcephaly. He had micrognathia, beaked nose, small mouth, loss of lateral eyebrows and high arched palate (Figure 1A-C). He had sloping shoulders, thin extremities, reduced muscle bulk and scanty subcutaneous fat. He had severe gingivitis and myopia. He was Tanner stage IV but had no facial hair and scant axillary and pubic hair. He had some limitation of movement of full extension of the elbows, knees and hips. He also had a short right index finger and incurved third toes (Figure 1D, E).

His fasting and two-hour post-prandial blood glucose values were normal (93 mg/dL and 112 mg/dL, respectively). He had normal serum total cholesterol (149 mg/dL), triglycerides (39 mg/dL), and high-density lipoprotein (HDL) cholesterol (45 mg/dL). His serum calcium (9.5 mg/dL; normal range: 8.4-10.2 mg/dL), phosphorus (3.75 mg/dL; normal range: 2.7-4.5 mg/dL); magnesium (2.11 mg/dL; normal range: 1.7-2.56 mg/dL); and alkaline phosphatase (40.7 IU/L; normal range: 40-129 IU/L) were normal. His serum parathyroid hormone was elevated (111.5 pg/mL; normal range: 9-55 pg/mL) and 25 hydroxy-vitamin D level was low (12.3 ng/mL; normal range: 30-70 ng/mL). He had normal serum adrenocorticotrophic hormone (ACTH: 28.1 pg/mL; normal range: 7.2-63 pg/mL), cortisol (15.7 µg/dL; normal range: 3.7-19.4 µg/dl); thyroid stimulating hormone (TSH: 2.12 µIU/mL; normal range: 0.35-5.01 µIU/mL); free thyroxine (9.87 pmol/L; normal range:

9.10-23.80 pmol/L); luteinizing hormone (LH: 3.25 mIU/mL; normal range: 1.14-8.75 mIU/mL), follicle stimulating hormone (FSH: 3.68 mIU/mL; normal range: 0.95-11.95 mIU/mL) and testosterone (3.22 ng/mL; normal range: 2.41-8.27 ng/mL) concentrations. His serum growth hormone (GH) was 1.35 ng/mL (normal values: 0.4-2.47 ng/mL) but insulin-like growth factor-1 (IGF-1) concentration repeated twice were 73.6 and 76.5 ng/mL (-3.33 SD; normal range: 99-655 ng/mL), and were extremely low. A 240-minute 1 mg intramuscular glucagon (GlucaGen, Novo Nordisk) stimulation test at age 24 years revealed peak stimulated serum GH concentration of 3.23 ng/mL at 120 minutes from the baseline value of 0.51 ng/mL.

Roentgenograms of the wrist revealed bone age corresponding to the chronological age of 20 years. A dual-energy X-ray absorptiometry (DEXA; Hologic Discovery A; Hologic, Inc., Waltham, MA) revealed an overall Z score of -4.78 (height adjusted Z score according to Zemel *et al*. (8), -2.6), lumbar 1-4 vertebral Z score of -4.6 (height adjusted, -2.8), and left femoral neck Z score of -4.5 (height adjusted, -3.4). There was no history of bone fractures. His total body fat was 24.4%, with arm fat of 21.4%, leg fat of 27.6% and truncal fat of 22.9%. Whole body magnetic resonance imaging revealed near normal body fat distribution (Figure 1F-I). Echocardiography showed trace mitral valve regurgitation. Audiometry showed moderate bilateral high frequency (8000 Hz) sensorineural hearing loss (Figure 1J).

He died recently due to suspected food poisoning after presenting to the local hospital with vomiting and dehydration. The clinical or laboratory data for this admission are not available.

His parents were first cousins (Figure 2A). The mid-parental height was 172 cm. One of his younger sisters was similarly affected and he had four younger healthy sisters and one healthy brother, all of whom were of average height and weight (Figure 2A).

Patient J100.5: This 18-year-old girl had developmental dysplasia of the hips requiring surgery at 7 and 12 months of age. At the age of five years, poor weight gain, short stature and muscle weakness were noted. She achieved menarche at 12 years and had irregular menstrual cycles. She had a high-pitched voice. Her height was 149 cm (1.2 percentile; z score -2.3), weight was 29.5 kg (z score -3.8) with a BMI of 13.3 kg/m^2 (z score -5.0) and occipito-frontal circumference was 50.5 cm (z score -3.6) denoting microcephaly. She had micrognathia, beaked nose, small mouth, loss of lateral eyebrows and high arched palate. She had thin and slender extremities, reduced muscle bulk, and scanty subcutaneous fat. Her breast and pubic hair development were Tanner stage III but she had scant axillary hair.

Her fasting blood glucose was 94 mg/dL and two-hour post-prandial blood glucose was 89 mg/dL. She had normal serum total cholesterol (163 mg/dL), triglycerides (48 mg/dL), HDL cholesterol (60 mg/dL), serum calcium (9.3 mg/dL), phosphorus (3.9 mg/dL), magnesium (1.99 mg/dL), alkaline phosphatase (40.6 IU/L), TSH (1.62 µIU/mL), free thyroxine (9.52 pmol/L), ACTH (24.5 pg/mL), cortisol (18.5 µg/dL), LH (3.36 mIU/mL; normal range: 1.6-12.4 mIU/mL), FSH (3.3 mIU/mL; normal range Mid-follicular phase: 2.5-10.2 mIU/mL) and estradiol levels (113.4 pg/mL; normal range Mid-follicular phase: 27-123 pg/mL). Her serum parathyroid hormone level was high (81.7 pg/mL) and 25 hydroxy-vitamin D level was low (8.5 ng/mL). Her serum GH level was 1.96 ng/mL (normal

values 1-8 ng/mL) but IGF-1 levels repeated twice were 46.6 and 46.7 ng/mL (-3.51 SD; normal range: 73-522 ng/mL), and were extremely low. A 240-minute 1 mg intramuscular glucagon (GlucaGen, Novo Nordisk) stimulation test at age 18 years revealed peak stimulated serum GH level of 3.83 ng/mL at 120 minutes from the baseline level of 1.37 ng/mL.

She had normal hearing on audiometry and normal echocardiogram. Her bone age corresponded to the chronological age of 16 years. A DEXA revealed an overall Z score of -3.2 (height-adjusted, -2.25), lumbar 1-4 vertebral Z score of -2.3 (height-adjusted, -1.5), left femoral neck Z score of -3.4 (height-adjusted, -2.9). There was no history of bone fractures. Her total body fat was 32.7%, with arm fat of 32.6%, leg fat of 43% and truncal fat of 26.6%. Her whole-body MRI revealed near normal subcutaneous and intra-abdominal fat. Follow up at age 18 years revealed that she had developed a seizure disorder, which was controlled by medications.

Methods

Genotyping: Genomic DNA was isolated from peripheral blood using the Easy-DNA kit (Invitrogen, Carlsbad, CA). Two affected (J100.3 and J100.5) and two unaffected (J100.4, J100.8) subjects (Figure 2A) underwent whole exome sequencing using the SureSelect Human All Exon V4 kit on the Illumina platform. Sequencing read length was paired-end 2x100 bp. Sequences were aligned to the human reference genome b37. The mean coverage of the targeted regions for J100.3, J100.4, J100.5, and J100.8 were 99, 95, 126, and 88-fold, respectively, with >98% bases covered by >10-fold reads in all samples. Genetic variations were called using the Genome Analysis Toolkit (9) and annotated

using SnpEff (10). Because of parental consanguinity and 2 of the 7 siblings being affected, we hypothesized a homozygous variant was most likely. Thus, we mapped the disease gene by a combination of two approaches. First, we first searched for runs of homozygosity (ROH) greater than 1 MB and shared by the two affected but not by the two unaffected using BCFtools/RoH (11). Second, we filtered for rare missense, nonsense, splicing, or frameshift homozygous variants shared by the two affected but not by the two unaffected with minor allele frequency (MAF) less than 0.01 in the 1000 Genomes Project (http://www.internationalgenome.org/), genome aggregation database (gnomAD v2.1.1; http://gnomad.broadinstitute.org/), and the Greater Middle East (GME) Variome Project database (http://igm.ucsd.edu/gme/). Variants with Genomic Evolutionary Rate Profiling (GERP)++ score (12) greater than 1.0 and Combined Annotation Dependent Depletion (CADD) score (13) greater than 10 were considered. We considered missense variants predicted to be "probably damaging" by Polymorphism Phenotyping v2 (PolyPhen2, HumDiv; http://genetics.bwh.harvard.edu/pph2/). We also performed Sanger sequencing to confirm segregation of the candidate variants within the pedigree.

mRNA Expression Studies: In order to study the tissue expression of *PRRT3* mRNA, we designed primers in both the 5' and 3' regions of the gene specific to PRRT3. The human normal cDNA tissue array was obtained from Origene (TissueScan, Rockville, MD).

Results

The ROH analysis revealed a total of 22.1 Mb stretches of homozygous segments consisting of 5 regions greater than 1 Mb in length, which were shared by the two affected siblings but not by the two unaffected siblings. Out of the 5 regions, there was one significant ROH on chromosome 3 spanning ~15.7 Mb (9,896,351 – 25,632,113) (Figure 2B). There was no indication of copy number variation in the region according to ExomeDepth (14). There were only two candidate variants with minor allele frequency < 0.01 in the ROH: the *PRRT3* variant on chromosome 3 and a *GPR110* variant on chromosome 6. The *GPR110* variant had a low PolyPhen score of 0.618, which failed the PolyPhen criterion, and furthermore, upon Sanger sequencing of all the family members, it did not segregate with the phenotype in our family. The unaffected mother was homozygous for the *GPR110* variant. The *PRRT3* homozygous variant, NC_000003.11:g.9989677C>T leading to a c.1180G>A nucleotide change and corresponding protein change, NP_997234.4: p.Glu394Lys, passed the filtering criteria (Figure 2). This variant (rs909458664) was not seen in gnomAD or GME; however, there were 3 heterozygotes among 62,784 individuals in TOPMed database freeze5 (https://bravo.sph.umich.edu/freeze5/hg38/). Sanger sequencing further confirmed the segregation of this variant in the family (Figure 2A, B). No pathogenic variants were found in either of the affected subjects in progeria or progeroid syndrome genes, such as, *LMNA, ZMPSTE24, BANF1, RECQL2, RECQL4, BLM, POLD1, POLR3A, WRN, ERCC4, ERCC6, ERCC8, TERT1, TERC, DKC1, AKT1P, SPRTN, XPA, XPB, XPC, and XPG* (15).

PRRT3 belongs to the family of proline-rich proteins containing several repeats of a short proline-rich sequence. PRRT3 has close homology with PRRT1, PRRT2 and

PRRT4, which are much smaller proteins (Figure 3A). However, the precise molecular function of PRRT3 remains to be determined. The central region of all PRRT proteins seems to be highly conserved which may suggest similar functions of these proteins. Recently, variants in *PRRT2* have been reported to cause episodic kinesigenic dyskinesia-1 (16). The glutamic acid at position 394 of PRRT3 is highly conserved across species (Figure 3B).

RNA expression studies using the primers in both the 5' and 3' regions of the gene specific to PRRT3 (Fig. 3A) revealed the highest relative expression in the pituitary, followed by muscle, pancreas, rectum and tonsil (Figure 3C). Other tissues, including the brain, showed low level of expression (C_t value ≥ 30)(Supplementary Table 1)(17).

Based on the secondary structure prediction of the human PRRT3-long form, we show the possible protein insertion in the membrane (Figure 3D) with the amino-terminus being intracellular while carboxy-terminus is extracellular. The variant p.E394K is in the coiled-coil region of the long isoform, near the cell membrane, but does not affect the short isoform (Figure 3E).

Discussion:

Given the strong conservation of PRRT3 to other proteins of the PRRT family, some functional clues can be derived. Just like PRRT2, PRRT3 could also be involved in exocytosis, transporting intracellular molecules to cell exterior on demand (18, 19). Preliminary observations showing co-localization of Prrt3 and synaptophysin (20) support its role in vesicle exocytosis in pituitary cells as well as in neurons (21). Preliminary phenotyping of the homozygous *Prrt3* knock out mice, with deletion of the entire *Prrt3*

affecting the expression of both the isoforms, revealed small size and high mortality before 7 days of age (22). These observations suggest a critical role of PRRT3 in neurobiology and in sustaining life after birth. However, our patients, with a unique *PRRT3* homozygous missense variant, which likely affects the function of the long isoform partially, had milder phenotype than the knock out mice.

Our patients had several unique clinical features suggestive of progeroid syndrome, including short stature, microcephaly, mandibular hypoplasia, pointed nose, shrill voice, severe osteoporosis and loss of hair from eyebrows. According to Biller *et al*. (23), a baseline serum IGF-1 level < 2 SD score, or < 77 ng/mL has a 100% specificity and 46% sensitivity for diagnosis of GH deficiency. In both our patients, serum IGF-1 levels were below 3 SD score and < 77 ng/mL, thus diagnostic of GH deficiency. Low serum IGF-1 levels in our patients are unlikely to be due to malnutrition as there was no evidence of malnutrition in the affected patients who had normal levels of serum protein, albumin and lipids. The low BMI in our patients were part of the novel autosomal recessive syndrome. Furthermore, both the patients had low serum GH response on glucagon stimulation test, especially considering that they received a fixed dose of 1 mg of glucagon despite their low body weights of 31 kg and 29.3 kg, suggesting mild GH deficiency (24, 25). The expression of *PRRT3* mRNA is also observed in the mouse inner ear hair cells (26) and may explain high frequency hearing loss in the proband. However, patient J100.5 did not have hearing loss. Both the patients had vitamin D deficiency and secondary hyperparathyroidism, which along with mild GH deficiency may be contributing to osteoporosis and short stature. Interestingly, despite mild GH deficiency, the bone age was not delayed in either of the affected subjects.

Each of the previously reported progeroid syndromes displays only a subset of the features of normal aging (27-30). In many patients, accelerated aging, driven by genetic variants, begins early in childhood resulting in profound growth retardation and poor sexual development. The sexual development of our patients appears near normal but the male had no facial hair and the female had irregular menstrual cycles. Both of them had normal serum gonadotropin levels, and the male had normal testosterone and the female had normal estradiol levels. The reproductive capabilities of our patients are not known. Although physical examination suggested scant subcutaneous fat in the extremities of both our patients, the objective evaluation of regional body fat by DEXA scans and whole-body magnetic resonance imaging did not support a lipodystrophic phenotype.

One limitation of the current study is that there is only one nuclear family available. Moreover, the function of PRRT3 is largely unknown and there is no human disorder reported to be associated with it yet. As such, the p.Glu394Lys variant is only classified as of uncertain significance by the American College of Medical Genetics and Genomics and the Association for Molecular Pathology guidelines (31). It meets the criterion of absence in population databases (PM2), but the *in silico* predictions are conflicting. It is well conserved ($GERP^{++}$ = 4.89), predicted to be probably damaging by some algorithms (CADD = 25.2; PolyPhen = 0.994) but likely benign by other algorithms (SIFT = 0.071; REVEL = 0.095). However, its co-segregation with phenotype constitutes a moderate evidence of being pathogenic. The genotype-phenotype co-segregation probability proposed by Jarvik and Browning (32) can be calculated as $N = (1/4) \times (3/4)^5$ and is $< 1/16$, where the first and second factors correspond to the affected and unaffected,

respectively. Based on the Clinical Genome Resource classification method (33), the strength of evidence is “limited” with ~2 points from the genetic evidence. Identification of a second family with similar phenotype caused by biallelic variants in *PRRT3* would confirm our discovery and shed more light on the function of the gene. We have made a submission (ID:50378) to GeneMatcher (34) but so far, have not found any other pedigree with *PRRT3* biallelic variants.

Another limitation is that we only performed whole exome instead of whole-genome sequencing. There is always a likelihood that the disease-causing variant lies in the non-coding regions. Moreover, there can be multiple genetic causes of underlying complex phenotypes such as progeria, particularly in a consanguineous pedigree where there are long stretches of homozygous regions in the affected. In the current study, we manually checked that there was no pathogenic variant in the progeroid syndrome genes (15) in either of the affected subjects and none of the causal genes lied in a homozygous region shared by the two affected but heterozygous in the unaffected.

We conclude that the homozygous p.Glu394Lys variant in *PRRT3* may be associated with a novel autosomal recessive, progeroid syndrome with short stature, mandibular hypoplasia, osteoporosis, short eyebrows and mild GH deficiency. Our report extends the spectrum of progeroid syndromes and elucidates important functions of PRRT3 in human biology including secretion of GH from the pituitary.

Acknowledgments:

We thank Carmel Tovar and Mary Tunison for illustrations and mRNA expression data; the McDermott Center Sequencing and Bioinformatics Cores for sequencing and analysis.

Author Contributions: AG oversaw the study, coordinated the work and prepared the manuscript, which was reviewed, edited and approved by all authors. HE-S, MA, KA-R, ME-K, and KA examined the patients and the family members, collected blood samples, and performed other laboratory tests. CX and ZZ analyzed the data from whole-exome sequencing. AKA performed tissue expression studies.

References:

1. Yu CE, Oshima J, Fu YH, Wijsman EM, Hisama F, Alisch R, Matthews S, Nakura J, Miki T, Ouais S, Martin GM, Mulligan J, Schellenberg GD. Positional cloning of the Werner's syndrome gene. Science. 1996;272(5259):258-62.
2. Eriksson M, Brown WT, Gordon LB, Glynn MW, Singer J, Scott L, Erdos MR, Robbins CM, Moses TY, Berglund P, Dutra A, Pak E, Durkin S, Csoka AB, Boehnke M, Glover TW, Collins FS. Recurrent de novo point mutations in lamin A cause Hutchinson-Gilford progeria syndrome. Nature. 2003;423:293-8.
3. Garg A, Subramanyam L, Agarwal AK, Simha V, Levine B, D'Apice MR, Novelli G, Crow Y. Atypical progeroid syndrome due to heterozygous missense LMNA mutations. J Clin Endocrinol Metab. 2009;94(12):4971-83.

10.1210/jc.2009-0472. PubMed PMID: 19875478; PMCID: 2795646.
4. Novelli G, Muchir A, Sangiuolo F, Helbling-Leclerc A, D'Apice MR, Massart C, Capon F, Sbraccia P, Federici M, Lauro R, Tudisco C, Pallotta R, Scarano G, Dallapiccola B, Merlini L, Bonne G. Mandibuloacral dysplasia is caused by a mutation in LMNA-encoding lamin A/C. Am J Hum Genet. 2002;71(2):426-31.
5. Agarwal AK, Fryns JP, Auchus RJ, Garg A. Zinc metalloproteinase, *ZMPSTE24*, is mutated in mandibuloacral dysplasia. Hum Mol Genet. 2003;12(16):1995-2001.
6. Weedon MN, Ellard S, Prindle MJ, Caswell R, Lango Allen H, Oram R, Godbole K, Yajnik CS, Sbraccia P, Novelli G, Turnpenny P, McCann E, Goh KJ, Wang Y, Fulford J, McCulloch LJ, Savage DB, O'Rahilly S, Kos K, Loeb LA, Semple RK, Hattersley AT. An in-frame deletion at the polymerase active site of POLD1 causes a multisystem disorder with lipodystrophy. Nat Genet. 2013;45(8):947-50.
7. Wambach JA, Wegner DJ, Patni N, Kircher M, Willing MC, Baldridge D, Xing C, Agarwal AK, Vergano SAS, Patel C, Grange DK, Kenney A, Najaf T, Nickerson DA, Bamshad MJ, Cole FS, Garg A. Bi-allelic POLR3A Loss-of-Function Variants Cause Autosomal-Recessive Wiedemann-Rautenstrauch Syndrome. Am J Hum Genet. 2018.

8. Zemel BS, Kalkwarf HJ, Gilsanz V, Lappe JM, Oberfield S, Shepherd JA, Frederick MM, Huang X, Lu M, Mahboubi S, Hangartner T, Winer KK. Revised reference curves for bone mineral content and areal bone mineral density according to age and sex for black and non-black children: results of the bone mineral density in childhood study. J Clin Endocrinol Metab. 2011;96(10):3160-9.
9. McKenna A, Hanna M, Banks E, Sivachenko A, Cibulskis K, Kernytsky A, Garimella K, Altshuler D, Gabriel S, Daly M, DePristo MA. The Genome Analysis Toolkit: a MapReduce framework for analyzing next-generation DNA sequencing data. Genome Res. 2010;20(9):1297-303.
10. Cingolani P, Platts A, Wang le L, Coon M, Nguyen T, Wang L, Land SJ, Lu X, Ruden DM. A program for annotating and predicting the effects of single nucleotide polymorphisms, SnpEff: SNPs in the genome of Drosophila melanogaster strain w1118; iso-2; iso-3. Fly (Austin). 2012;6(2):80-92.
11. Narasimhan V, Danecek P, Scally A, Xue Y, Tyler-Smith C, Durbin R. BCFtools/RoH: a hidden Markov model approach for detecting autozygosity from next-generation sequencing data. Bioinformatics. 2016;32(11):1749-51.
12. Davydov EV, Goode DL, Sirota M, Cooper GM, Sidow A, Batzoglou S. Identifying a high fraction of the human genome to be under selective constraint using GERP++. PLoS Comput Biol. 2010;6(12):e1001025.
13. Kircher M, Witten DM, Jain P, O'Roak BJ, Cooper GM, Shendure J. A general framework for estimating the relative pathogenicity of human genetic variants. Nat Genet. 2014;46(3):310-5.
14. Plagnol V, Curtis J, Epstein M, Mok KY, Stebbings E, Grigoriadou S, Wood NW, Hambleton S, Burns SO, Thrasher AJ, Kumararatne D, Doffinger R, Nejentsev S. A robust model for read count data in exome sequencing experiments and implications for copy number variant calling. Bioinformatics. 2012;28(21):2747-54.
15. Carrero D, Soria-Valles C, Lopez-Otin C. Hallmarks of progeroid syndromes: lessons from mice and reprogrammed cells. Disease models & mechanisms. 2016;9(7):719-35.
16. Chen WJ, Lin Y, Xiong ZQ, Wei W, Ni W, Tan GH, Guo SL, He J, Chen YF, Zhang QJ, Li HF, Lin Y, Murong SX, Xu J, Wang N, Wu ZY. Exome sequencing identifies truncating mutations in PRRT2 that cause paroxysmal kinesigenic dyskinesia. Nat Genet. 2011;43(12):1252-5.
17. Supplementary Data From: Garg A, El-Shanti H, Xing C, Zhou Z, Abujbara M, Al-Rashed K, El-Khatib M, Ajlouni K, Agarwal AK. A novel syndrome with short stature, mandibular hypoplasia and osteoporosis may be associated with a PRRT3 variant [Internet]2020 [cited Deposited Sep 18, 2019]. Available from: https://utswmed-ir.tdl.org/handle/2152.5/7263.
18. Valtorta F, Benfenati F, Zara F, Meldolesi J. PRRT2: from Paroxysmal Disorders to Regulation of Synaptic Function. Trends Neurosci. 2016;39(10):668-79.
19. Matt L, Kirk LM, Chenaux G, Speca DJ, Puhger KR, Pride MC, Qneibi M, Haham T, Plambeck KE, Stern-Bach Y, Silverman JL, Crawley JN, Hell JW, Diaz E. SynDIG4/Prrt1 Is Required for Excitatory Synapse Development and Plasticity Underlying Cognitive Function. Cell reports. 2018;22(9):2246-53.
20. Yamamato I, Konno K, Yamamato T, Watanabe M, Kubo Y. Expression patterns of an orphan metabotropic receptor for Prrt3 in mice. J Physiol Sci. 2014;64:S118.
21. Sudhof TC, Rizo J. Synaptic vesicle exocytosis. Cold Spring Harb Perspect Biol. 2011;3(12).
22. Yamamato T, Hattori S, Kiyonari H, Nakao K, Miyakawa T, Kubo Y. Comprehensive behavioral test battery analyses of the gene targeted mice of Prrt3, an orphan metabotropic receptor. J Physiol Sci. 2014;64:S118.
23. Biller BM, Samuels MH, Zagar A, Cook DM, Arafah BM, Bonert V, Stavrou S, Kleinberg DL, Chipman JJ, Hartman ML. Sensitivity and specificity of six tests for the diagnosis of adult GH deficiency. J Clin Endocrinol Metab. 2002;87(5):2067-79.
24. Chesover AD, Dattani MT. Evaluation of growth hormone stimulation testing in children. Clin Endocrinol (Oxf). 2016;84(5):708-14.

25. Yuen KCJ, Biller BMK, Radovick S, Carmichael JD, Jasim S, Pantalone KM, Hoffman AR. American Association of Clinical Endocrinologists and American College of Endocrinology Guidelines for Management of Growth Hormone Deficiency in Adults and Patients Transitioning from Pediatric to Adult Care. Endocr Pract. 2019;25(11):1191-232.
26. Scheffer DI, Shen J, Corey DP, Chen ZY. Gene Expression by Mouse Inner Ear Hair Cells during Development. J Neurosci. 2015;35(16):6366-80.
27. Oshima J, Sidorova JM, Monnat RJ, Jr. Werner syndrome: Clinical features, pathogenesis and potential therapeutic interventions. Ageing Res Rev. 2017;33:105-14.
28. Hennekam RC. Hutchinson-Gilford progeria syndrome: review of the phenotype. Am J Med Genet A. 2006;140(23):2603-24.
29. Paolacci S, Bertola D, Franco J, Mohammed S, Tartaglia M, Wollnik B, Hennekam RC. Wiedemann-Rautenstrauch syndrome: A phenotype analysis. Am J Med Genet A. 2017. Epub 2017/04/28.
30. Simha V, Agarwal AK, Oral EA, Fryns JP, Garg A. Genetic and phenotypic heterogeneity in patients with mandibuloacral dysplasia-associated lipodystrophy. J Clin Endocrinol Metab. 2003;88(6):2821-4.
31. Richards S, Aziz N, Bale S, Bick D, Das S, Gastier-Foster J, Grody WW, Hegde M, Lyon E, Spector E, Voelkerding K, Rehm HL, Committee ALQA. Standards and guidelines for the interpretation of sequence variants: a joint consensus recommendation of the American College of Medical Genetics and Genomics and the Association for Molecular Pathology. Genet Med. 2015;17(5):405-24.
32. Jarvik GP, Browning BL. Consideration of Cosegregation in the Pathogenicity Classification of Genomic Variants. Am J Hum Genet. 2016;98(6):1077-81.
33. Strande NT, Riggs ER, Buchanan AH, Ceyhan-Birsoy O, DiStefano M, Dwight SS, Goldstein J, Ghosh R, Seifert BA, Sneddon TP, Wright MW, Milko LV, Cherry JM, Giovanni MA, Murray MF, O'Daniel JM, Ramos EM, Santani AB, Scott AF, Plon SE, Rehm HL, Martin CL, Berg JS. Evaluating the Clinical Validity of Gene-Disease Associations: An Evidence-Based Framework Developed by the Clinical Genome Resource. Am J Hum Genet. 2017;100(6):895-906.
34. Sobreira N, Schiettecatte F, Valle D, Hamosh A. GeneMatcher: a matching tool for connecting investigators with an interest in the same gene. Hum Mutat. 2015;36(10):928-30.
35. Rossi P, Sterlini B, Castroflorio E, Marte A, Onofri F, Valtorta F, Maragliano L, Corradi A, Benfenati F. A Novel Topology of Proline-rich Transmembrane Protein 2 (PRRT2): Hints for an Intracellular Function at the Synapse. J Biol Chem. 2016;291(12):6111-23.

Figure Legends:

Figure 1. Clinical features of Patient 1 (J100.3) with short stature, mandibular hypoplasia, osteoporosis and short eyebrows progeroid syndrome. Anterior (A), and left lateral (B) views of the Patient 1 (at age 18) showing thin limbs with a paucity of subcutaneous (sc) fat on the trunk and extremities with normal hair on the scalp but lack of facial and body hair. C. Anterior view of the face of Patient 2 (J100.5) showing small mandible, beaked nose, and loss of lateral third of the eyebrows. D. Posterior view of Patient 2 showing thin limbs with paucity of subcutaneous fat on the extremities. E. Anterior view of the face of Patient 1 showing small mandible, beaked nose, and loss of lateral third of the eyebrows and lack of facial hair on the upper lip, chin and cheeks. F. Dorsal view of the right hand of Patient 1 showing short index finger. G. Dorsal view of the right foot of Patient 1 showing incurved third toe. H. Sagittal MRI of the head and neck through midline of Patient 1 shows normal amount of sc fat in the scalp, neck and upper chest. I. Axial MRI of the chest at the level of the base of the heart of Patient 1 showing normal sc fat anteriorly and posteriorly. J. Axial MRI of the mid-thigh of Patient 1 showing normal amount of sc and intermuscular fat. K. Axial MRI of the abdomen at the level of the kidneys of Patient 1 showing normal amount of fat in the sc, intraperitoneal, and retroperitoneal (perinephric) region. L. Audiometry of Patient 1 showing moderate high frequency (8,000 Hz) hearing loss in both the ears. Hearing level below 20 dB at a frequency is considered hearing loss.

Figure 2. J100 Pedigree and the pathogenic variant in PRRT3. A. J100 pedigree. The circles denote females and squares males. Subjects with homozygous c.1180G>A *PRRT3* variant are shown as A/A; heterozygotes as G/A; with the wild type alleles as G/G under the symbols. Symbols filled with black color indicate affected subjects with progeroid syndrome, and unfilled symbols indicate unaffected subjects. A slanted arrow indicates the proband, and asterisks indicate subjects who underwent whole exome sequencing. Double horizontal line indicate consanguinity among parents (first cousins). Data are also included for height, weight, body mass index (BMI) and occipital-frontal circumference (OFC) for each participant. For the children and proband (assuming his age to be 19.9 years), z-scores were calculated from the CDC data (https://www.cdc.gov/growthcharts/percentile_data_files.htm.). For the adults, z-score for height was calculated from https://tall.life/height-percentile-calculator-age-country/. B. Region of homozygosity on chromosome 3 spanning ~15.7 Mb (9,896,351 – 25,632,113 bp), shared by the two affected individuals (J100.3 and J100.5) but not by the two unaffected subjects (J100.4 and J100.8). The top line represents the markers with alternate homozygous genotypes; the bottom line corresponds to the heterozygous genotypes. The rectangles highlight the homozygous regions— red if the regions are shared by more than one subject, grey if the regions are private to one subject. C. The human *PRRT3* gene contains four exons and three introns. The hatched boxes indicate untranslated regions. The arrow indicates the direction of the coding transcript. The variant g.9989677C>T; c.1180G>A is present in exon 4 of the *PRRT3*. D. Sequence electropherogram from Sanger sequencing of *PRRT3* showing wild type sequence E.

Heterozygous c.1180G>A (p.Glu394Lys) *PRRT3* variant in an unaffected subject and

F. Homozygous c.1180G>A (p.Glu394Lys) *PRRT3* variant in an affected subject.

Figure 3. Alignment of various PRRT proteins, conservation of the mutated glutamic acid across species, tissue expression of *PRRT3* mRNA and schematic of the predicted human PRRT3 isoforms insertion in the cell membrane. A. Snapshot of the protein alignment of PRRT 1-4 using NCBI COBALT multiple alignment tool. The highly conserved regions for these isoforms are shown in red. The conserved region spans between amino acids 216-461 of PRRT3. The primers used for RT-qPCR were designed in the 5' and 3' region of the gene so that they specifically amplify PRRT3. The amplified product using these primer sets were confirmed by Sanger sequencing. GenBank Acc#; PRRT1 - NM_030651.3 → NP_085154.3; PRRT2 - NM_145239.2 → NP_660282.2; PRRT3 - NM_207351.4 → NP_997234.3; PRRT4 - NM_001114726.2 → NP_001108198.2. B. Alignment of partial PRRT3 amino acid sequences from the human (H. Sapiens; NP_997234.3), chimpanzee (P. troglodytes; XP_001149591.1), rhesus monkey (M. mulatta; XP_001091855.1), gray wolf (C. lupus, XP_005632236.1), cow (B. Taurus; XP_005222668.1), mouse (M. musculus; NP_766075.2), and rat (R. norvegicus; XP_003749857.1). The mutated residue glutamic acid (E) at position 394 (shown in red in bold font) is conserved amongst all the species. C. Expression of human *PRRT3* mRNA in various tissues. Shown are the tissues whose C_t values were below 30 for both 5' and 3' region primer sets. The relative expression of each tissue is compared to that of tonsil. Expression in the pituitary is 5 to 13 fold higher than that in the tonsil. D and E. Schematic for the human PRRT3 isoforms insertion in the plasma membrane based on secondary

structure prediction. *PRRT3* encodes a 981 amino acid protein (long-form) and a 421 amino acid protein (short-form). Both the isoforms share 390 amino-terminal amino acids and the long form has 591 unique carboxy-terminal amino acids and the short form has 31 unique carboxy-terminal amino acids. The modeling was performed using secondary structure prediction for human PRRT3 protein and a recent biochemical approach used for PRRT2 protein membrane insertion (35). The variant p.E394K (shown with a red X) resides in the intracellular part of PRRT3 and does not affect the short form.

Fig. 1

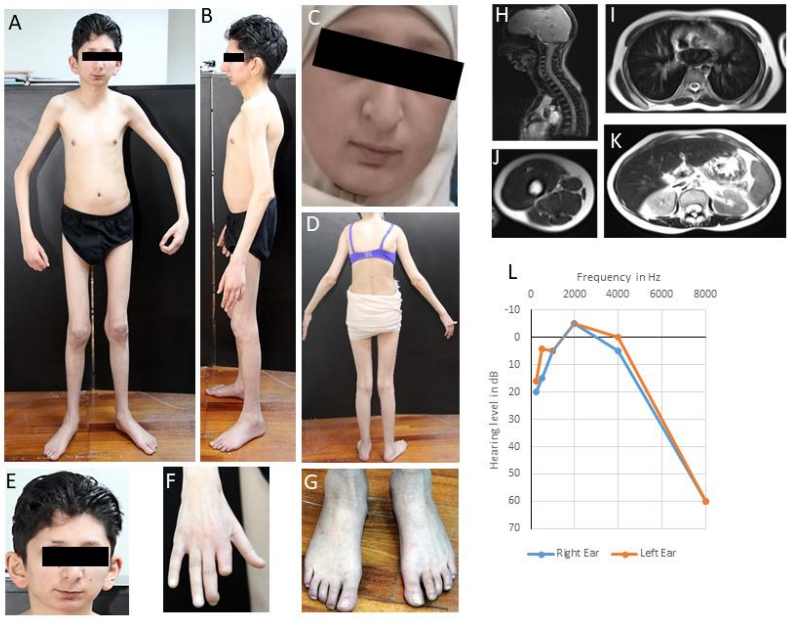

Fig. 2

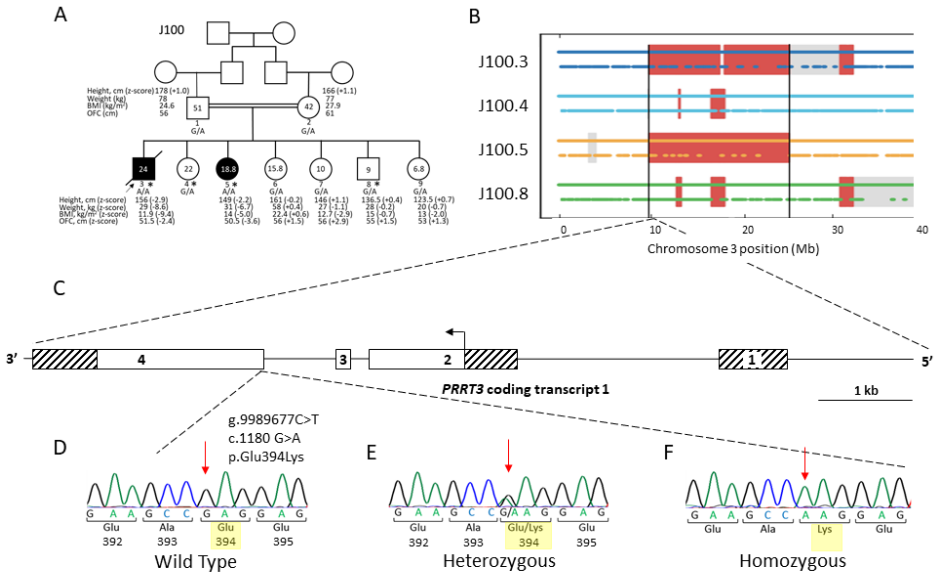

Fig. 3